

Principle and Experimental Verification of Novel Dual Driving Face Rotary Ultrasonic Motor

LU Xiaolong, HU Junhui*, YANG Lin, and ZHAO Chunsheng

*State Key Laboratory of Mechanics and Control of Mechanical Structures,
Nanjing University of Aeronautics and Astronautics, Nanjing 210016, China*

Received October 11, 2012; revised May 15, 2013; accepted June 13, 2013

Abstract: Existing rotary ultrasonic motors operating in extreme environments cannot meet the requirements of good environmental adaptability and compact structure at same time, and existing ultrasonic motors with Langevin transducers show better environmental adaptability, but size of these motors are usually big due to the radial arrangement of the Langevin transducers. A novel dual driving face rotary ultrasonic motor is proposed, and its working principle is experimentally verified. The working principle of the novel ultrasonic motor is firstly proposed. The 5th in-plane flexural vibration travelling wave, excited by the Langevin transducers around the stator ring, is used to drive the rotors. Then the finite element method is used in the determination of dimensions of the prototype motor, and the confirmation of its working principle. After that, a laser Doppler vibrometer system is used for measuring the resonance frequency and vibration amplitude of the stator. At last, output characteristics of the prototype motor are measured, environmental adaptability is tested and performance for driving a metal ball is also investigated. At room temperature and 200 V (zero to peak) driving voltage, the motor's no-load speed is 80 r/min, the stalling torque is 0.35 N · m and the maximum output power is 0.85 W. The response time of this motor is 0.96 ms at the room temperature, and it decreases or increases little in cold environment. A metal ball driven by the motor can rotate at 210 r/min with the driving voltage 300 V (zero to peak). Results indicate that the prototype motor has a large output torque and good environmental adaptability. A rotary ultrasonic motor owning compact structure and good environmental adaptability is proposed, and lays the foundations of ultrasonic motors' applications in extreme environments.

Key words: ultrasonic motor, piezoelectric transducer, dual driving face, in-plane flexural vibration mode

1 Introduction

Electromagnetic motors are widely utilized in many aspects for drive and control. However, in some special applications such as the precision driving and astronautic equipment, the ultrasonic motor which converts electric power into driving torque or pushing force via structural ultrasonic vibration is more competitive because of its higher motional resolution, quick response time and magnetic field free operation^[1-3]. Also, the ultrasonic motor does not need a gear system to reduce its speed, which makes it more reliable in and adaptable to the extreme operation environment like the cryogenic condition^[4-6].

The traditional traveling wave rotary ultrasonic motor has been broadly used, but bonding technology for piezoelectric layers' assembling limits its life time and

stability especially driven in extreme environment. Ultrasonic motors with Langevin transducers are widely investigated for its high reliability and large output power. HU, et al^[7-8], proposed a vibration excitation structure in which two longitudinal Langevin transducers are used to generate a travelling wave in a stator ring. A large rotating speed (3 500 r/min) is achieved and theoretical explanations are given. IULA, et al^[9-11], proposed a high-power travelling wave ultrasonic motor with several transducers, and its maximum speed and static torque are 116 r/min and 0.94 N · m, respectively. SATONBU, et al^[12], proposed an ultrasonic motor with symmetric hybrid transducers and pointed out the spring selection is the key to the motor's output torque. JIN, et al^[13], proposed an ultrasonic motor using a bar shaped transducer and its maximum torque and rotating speed are 0.25 N · m and 50 r/min, respectively. LIU, et al^[14-17], proposed a square type rotary ultrasonic motor with four driving feet. It has no-load speed of 71 r/min and maximum torque of 12.3 N · m at an exciting voltage of 200 V (root mean square value). Reported ultrasonic motors with Langevin transducers can provide rotation or linear motion^[18-22]. These researches provide the principles, structures, characteristics, design methods and

* Corresponding author. E-mail: ejhhu@nuaa.edu.cn

This project is supported by National Natural Science Foundation of China (Grant Nos. 51205203, 51275228, 51075212, 91123020), Science and Research Foundation, Nanjing University of Aeronautics and Astronautics (Grant Nos. 56YAH12015, NZ2010002, S0896-013), Innovation and Entrepreneurship Program of Jiangsu, and Priority Academic Program Development of Jiangsu Higher Education Institutions

modeling of this type of motor. However, the operation environment orientated design, which is very important for the motor's application has been rarely reported.

Inspired by the above reports, an ultrasonic motor owing compact size, large output torque and good environmental adaptability can be designed out by considering the following factors: (a) Langevin transducers should be employed instead of bonding technology for piezoelectric layers' assembling; (b) Spatial arrangement for the Langevin transducers should be reasonable for acquiring a compact structure of the motor; (c) Interface for driving the rotor should be more than one and its area should be large for improve the motor's mechanical characteristics; (d) No support bearing structure should be included for avoiding lubrication and thus improve the environmental adaptability in low temperature condition.

This paper proposes and designs a novel rotary ultrasonic motor with Langevin transducers, which has two driving faces in its stator ring for generating high driving torque. The stator consists of one stator ring operating at in-plane flexural mode and four Langevin transducers operating at 1st bending vibration mode. The two driving faces are conical and distributed in the middle of top and bottom surfaces of the stator ring. Two tapered rotors are assembled coaxially on the driving surfaces. The four Langevin transducers excite a travelling wave on each driving surface. Several elastic mountings are arranged at the vibration nodal positions of the Langevin transducers and distributed uniformly along the circumference of the motor. The stator drives the two rotors to rotate by the frictional force between the stator and rotors. The size of a prototype motor size is designed by the finite element method, and the prototype motor is fabricated and characterized.

2 Structure and Materials

The structure of the dual driving face rotary ultrasonic motor is shown in Fig. 1. It is composed of the base, stator, rotor A, rotor B, disk spring and nut. Rotor A has a tapered bottom with a long shaft in the center. Being similar to rotor A, rotor B is also tapered but with a center hole holding the shaft of rotor A. The stator is fastened on the base, and rotor A is pressed on the bottom conical driving face of the stator with the shaft through it. Rotor B is assembled with the common shaft to rotor A and pressed on the top conical driving surface. The disk spring is assembled on rotor B and pressed by the nut which is screwed to the end of the shaft. Thus, two tapered rotors are fitted on the two conical driving faces of the stator, and the preload between the rotor and stator can be adjusted by the disk spring. The conical driving faces can drive the rotors and their shaft to rotate without bearings. Additionally, PTFE composite material is utilized as the friction layer

adhered to the tapered faces of rotors, which makes the performance of the motor more stable and keeps the motor noise-free.

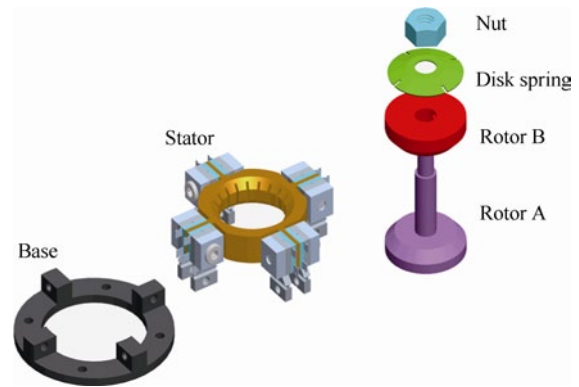
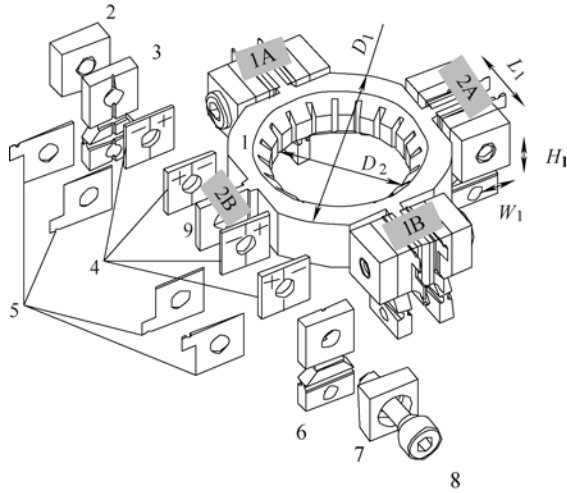


Fig. 1. Construction of the dual driving face ultrasonic motor

As shown in Fig. 2, the stator mainly consists of a stator ring with teeth distributed on the inner side uniformly, and four identical Langevin transducers (1A, 1B, 2A and 2B). And, the four Langevin transducers are assembled onto the projections on the outer side of the stator ring with equal separation. Each Langevin transducer is composed of one bottom cover, two elastic mountings, four bending mode piezoelectric plates, four electrodes, one front cover and one fastening screw. The four bending mode piezoelectric plates are stacked symmetrically about the corresponding projection and clamped by the screw. The size of the piezoelectric plate is $10\text{ mm} \times 10\text{ mm} \times 1\text{ mm}$ and there are two conversely polarized areas in each piezoelectric plate. The details about the elastic mounting are shown in Fig. 2(b). A trapezoidal part is used in the middle of the mounting for weakening the influence of fixed boundary on the transducer vibration. Besides that, four slots are cut out in the trapezoidal part for improving its elasticity while the stator is fixed to the base.

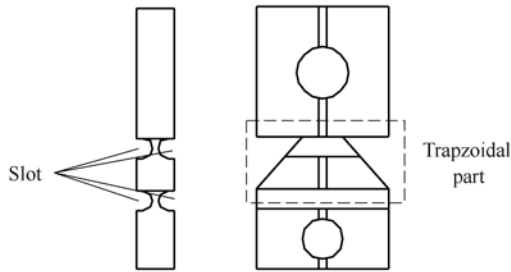
The piezoelectric plates in transducers 1A have opposite polarization directions to their counterparts in transducer 1B, and so are transducers 2A and 2B; the angular separation between transducers 1A and 2A is 90° , and so is that between transducers 1B and 2B. Thus, when applied with the same driving voltage, transducers 1A and 1B have opposite bending directions, and so are the transducers 2A and 2B. This arrangement can make the in-plane flexural working mode of the stator ring effectively excited.

Piezoelectric material in the transducers is PZT-8H. It has the piezoelectric constant d_{33} of 200 pC/N , electromechanical coupling factor k_{33} of 0.60, mechanical quality factor Q_m of 800, dielectric dissipation factor $\tan\delta$ of 0.5%, density of $7\,450\text{ kg/m}^3$ and Curie temperature T_c of 300°C . Phosphor bronze is chosen for making the stator ring and transducer metal parts, and Aluminum for making the rotor.



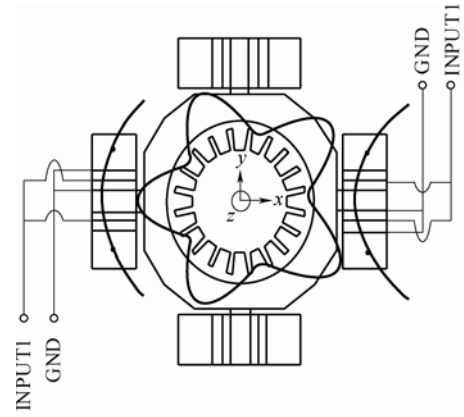
(a) Components of the whole stator

- 1. Stator ring; 2. Bottom cover; 3 & 6. Elastic mounting;
- 4. Piezoelectric plate; 5. Electrode; 7. Front cover;
- 8. Fastening screw; 9. Projection

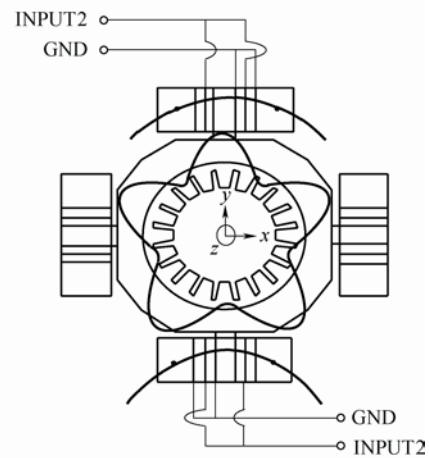


(b) Structure of the elastic mounting

Fig. 2. Configuration of the stator



(a) Sinusoidal AC voltage exciting



(b) Cosine AC voltage exciting

Fig. 3. Working principle of the stator

3 Working Principle

Our ultrasonic motor employs the 5th flexural in-plane vibration mode in the stator ring, which has five vibration wavelengths around its circumference, and its vibration direction is in the plane parallel to its top or bottom surface. As shown in Fig. 3(a), INPUT1 and GND denote the input sinusoidal AC voltage signal and the ground electrode, respectively. Transducers 1A and 1B vibrate in bending modes with 180° phase difference. Their driving frequencies are close to the natural frequency of the 5th flexural mode of the stator ring. A standing wave of the 5th flexural in-plane mode in the stator ring can be excited by the transducers. In Fig. 3(b), INPUT2 denotes the input cosine AC voltage applied to transducers 2A and 2B. With the same driving frequency, another standing wave of the 5th flexural mode is excited in the stator ring and it has a spatial phase difference of 1/4 wavelengths from the one excited by transducers 1A and 1B. When the two groups of transducers are applied with AC voltages out of temporal phase by 90°, these two standing waves in the stator ring can form a flexural travelling vibration wave in the *xy* plane of the stator ring. Therefore, the two rotors can be driven by the friction force at the interface between the stator and rotors.

4 FEM Based Design and Analyses

To excite the stator vibration efficiently, it is necessary to design the natural frequencies of the Langevin transducers' 1st order bending modes and the stator ring's 5th order flexural in-plane mode to be identical. Based on this principle, a series of FEM calculation and size adjustment are executed for determining the stator dimensions. Table 1 lists the final parameters shown in Fig. 2. The number of tooth in stator ring is 20. Calculated natural frequencies of the stator ring and transducers are around 51.8 kHz.

Parameter	Value	mm
Outer diameter of stator ring D_1	50	
Inner diameter of stator ring D_2	25	
Width of Langevin transducer W_1	10	
Length of Langevin transducer L_1	20.4	
Height of Langevin transducer H_1	10	

The vibration of the whole stator is analyzed at 51.8 kHz and 100 V (zero to peak) driving voltage, using the size

listed in Table 1, and Fig. 4 shows the result of vibration pattern of the stator when transducers 1A and 1B are driven. This figure confirms the vibration excitation principle of a standing wave in the stator ring.

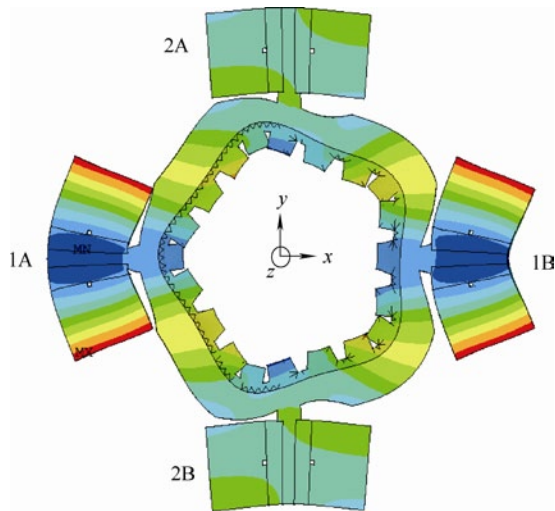


Fig. 4. Analyzed vibration pattern of the stator

5 Results and Discussion

A prototype motor is fabricated and assembled based on the above design, and its image is shown in Fig. 5. Its appearance size is $59\text{ mm} \times 59\text{ mm} \times 50\text{ mm}$. The rotor diameter is 30 mm with 45° taper degree and the friction material thickness is 0.2 mm . To effectively excite the travelling waves in the stator rings, the resonance frequencies of the 1st bending mode of the four transducers are experimentally tuned as closely as possible. A laser Doppler vibrometer system (PSV-300F-B) is used for measuring the vibration characteristics of the stator. As transducers 1A and 1B are driven by a 100 V (zero to peak) driving voltage and the other transducers are short circuited, the measured resonance frequency is 48.65 kHz . As transducers 2A and 2B are driven by a 100 V (zero to peak) driving voltage, and the other transducers are short circuited, the measured resonance frequency is 48.60 kHz . In the following experiments, unless otherwise specified, the driving frequency is set to 48.65 kHz , and the driving voltage is 100 V (zero to peak); the preload between the rotor and stator is about 100 N .

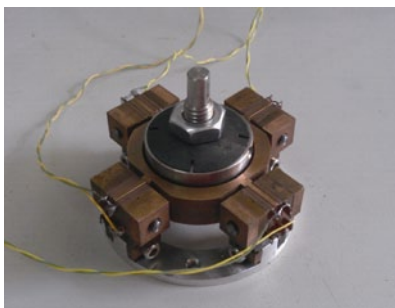
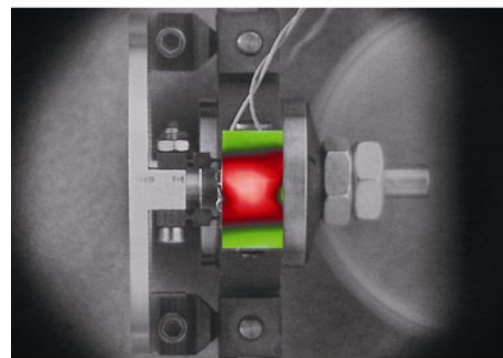
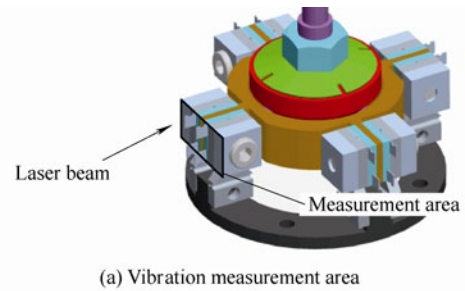


Fig. 5. Image of the prototype motor

5.1 Vibration characteristics

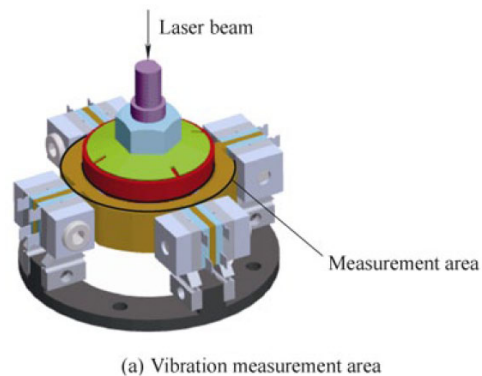
Measurement method and measured result of the bending vibration mode of the Langevin transducers are shown in Fig. 6. It can be seen that the Langevin transducers vibrate at the 1st bending mode, and the elastic mountings locate at the vibrating node positions. This result confirms the transducer vibration mode in the principle analysis and FEM result.



Magitude: ■ Negative(-) ■ Positive(+)
(b) Langevin transducer's vibration pattern

Fig. 6. Vibration measurement of the Langevin transducer

The out-of-plane standing wave vibration of stator ring's top surface is measured, and the measurement method and measured result are shown in Fig. 7. During the measurement, transducers 1A and 1B are driven and the other two short circuited. A standing wave with 5 wavelengths can be seen, which indirectly confirms the in-plane vibration mode of the driving surface in the principle analysis and FEM result. When the driving frequency and voltage are 48.65 kHz and 100 V (zero to peak), the measured out-of plane amplitude of the standing wave is 0.4 microns (zero to peak).



(a) Vibration measurement area

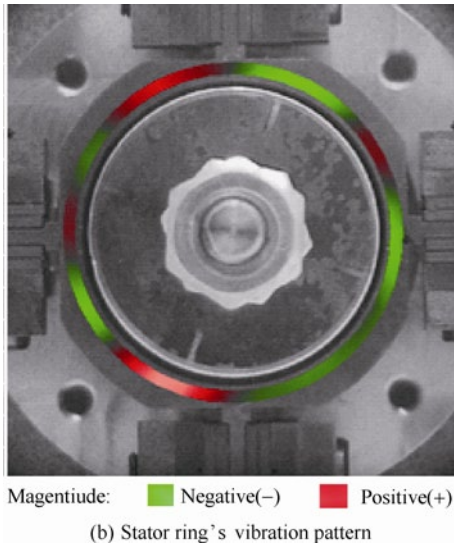


Fig. 7. Vibration measurement of the stator ring

5.2 Mechanical characteristics

Fig. 8 shows the measured output mechanical characteristics of the prototype motor at room temperature with driving frequency of 48.65 kHz and driving voltage of 200 V(zero to peak). It can be seen that the no-load speed is 80 r/min and stalling torque is 0.35 N · m, the maximum output power is about 0.85 W and the corresponding output torque is 0.2 N · m.

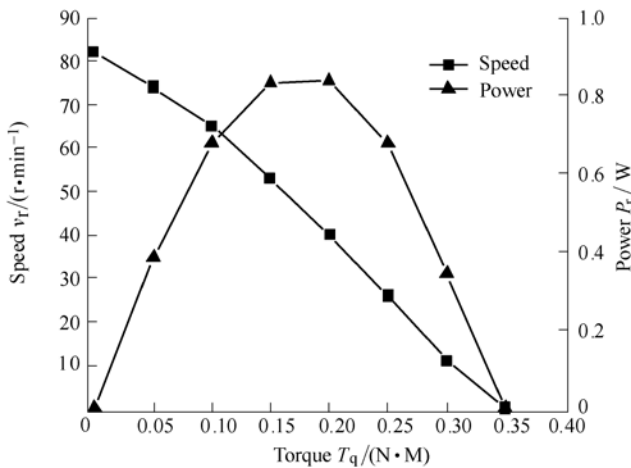


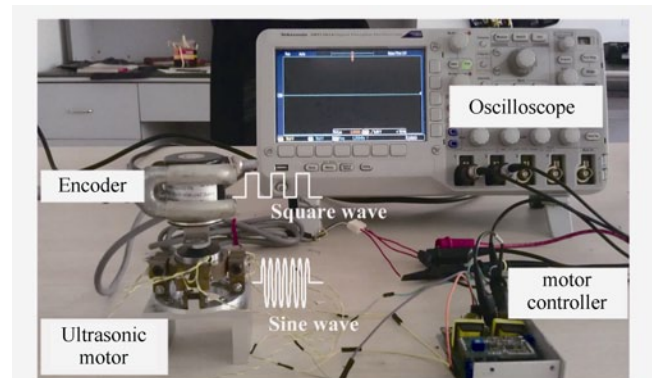
Fig. 8. Mechanical characteristics of the prototype motor

5.3 Response time

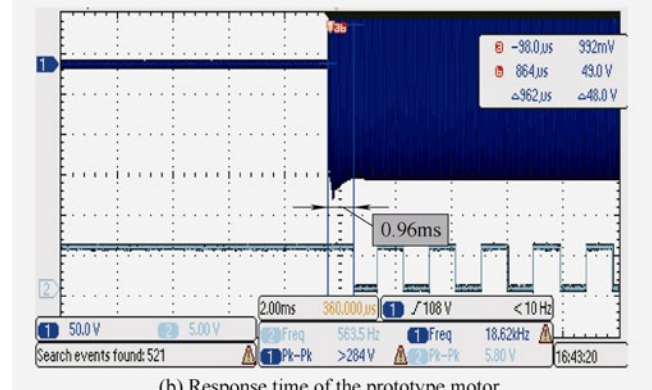
A measurement system for the response time of the prototype motor is built and shown in Fig. 9(a). In the system, a precise rotary encoder fixed to the shaft of the prototype motor is used for measuring the rotor's speed. A motor controller with tunable frequency is used to provide sinusoidal and cosine driving voltages to the motor. Oscilloscope DPO2014 is used to monitor the square wave from the rotary encoder and sinusoidal wave signal from the motor controller. Once the motor controller works, the

motor obtains the driving voltages and starts to rotate. Then, the rotary encoder outputs signal. DPO2014 records the signal waves. The run-up response time is defined as the time delay between the first sine wave and first square wave.

The results for the starting stage in room temperature are shown in Fig. 9(b). There are two signals named as No. 1 and No. 2, and No. 1 represents the sine wave and another represents the square wave. It can be seen that the measured run-up response time for this motor is 0.96 ms, which indicates the response of this type of motor is faster than our previous rotary ultrasonic motors^[5].



(a) Setup of the measurement system



(b) Response time of the prototype motor

Fig. 9. Measurement of the motor's response time

5.4 Response time at low temperature

The dependency of the response time on ambient temperature is also measured. In this measurement, the motor works at resonance and the driving voltage is set with different values. As shown in Fig. 10, as the temperature decreases, the response time decreases first and then increases, and it is the shortest at 0 °C. Faster response at low ambient temperature may be due to the elastic modulus increase of the PTFE composite friction layer, and slower response at much lower ambient temperature may be caused by the decrease of piezoelectricity, which lowers the vibration velocity of the stator driving faces. It is observed that the response time of this motor can be 0.45 ms when the ambient temperature is 0 °C, and the driving voltage is 250 V(zero to peak).

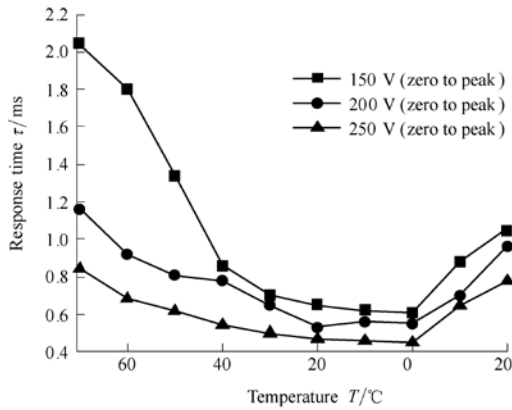


Fig. 10. Response time dependence of ambient temperature at different driving voltages

5.5 Driving a metal ball

Due to the conical driving faces, the motor can also be utilized for driving a metal ball without other assistant structures. In Fig. 11, an iron ball is put on the top conical driving face of the stator. This iron ball has a mass of 190 g and diameter of 36 mm. Its weight is used as the preload between the stator and iron ball. The ball's rotary speed versus driving voltage is measured at resonance and the result is plotted in Fig. 12. It is observed that the rotary speed increases as the driving voltage increases and their relationship is almost linear. The maximum rotary speed in the experimental range is about 210 r/min and the corresponding driving voltage is 300 V (zero to peak).

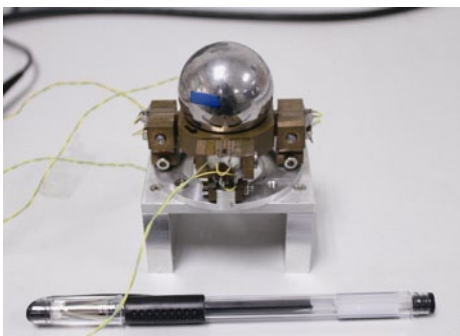


Fig. 11. Image of the stator driving a metal ball

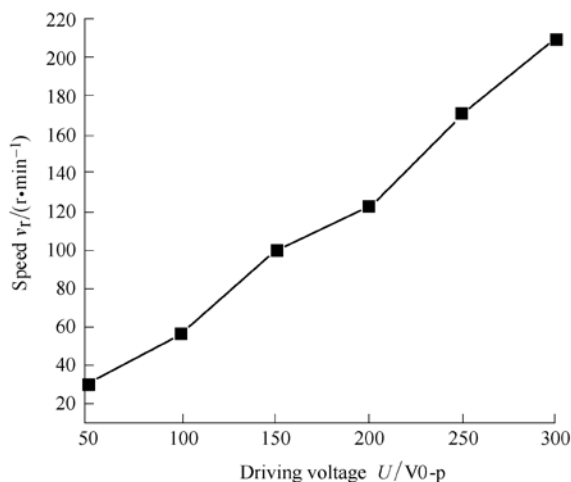


Fig. 12. Ball's rotating speed versus driving voltage

6 Conclusions

(1) A novel dual driving face rotary ultrasonic motor is proposed. This motor works in the in-plane flexural vibration mode, excited by four bending Langevin transducers. Two conical driving faces are used for driving tapered rotors without bearings. The stator vibration mode is simulated and the stator dimensions for best vibration excitation are determined by using the ANSYS software.

(2) A prototype motor is fabricated and the appearance size is 59 mm × 59 mm × 50 mm and its operating frequency is 48.65 kHz. The working principle is confirmed by measuring the vibration characteristics of the prototype motor.

(3) The motor's no-load speed is 80 r/min, the stalling torque is 0.35 N · m and the maximum output power is 0.85 W while operating at 48.65 kHz with driving voltage 200 V (zero to peak).

(4) The response time of this motor is 0.96 ms at room temperature at driving voltage 200 V (zero to peak) and resonance. Besides that, experimental measurement indicates that this prototype motor has good responses performance in low ambient temperature.

(5) This motor can also be used for driving a metal ball and the peak velocity value is 210 r/min with the driving voltage of 300 V (zero to peak).

References

- [1] SASHIDA T. Motor device utilizing ultrasonic oscillation: US, 4562374[P/OL]. 1984-05-16[1985-12-31]. <http://www.google.com.hk/patents?hl=zh-CN&lr=&vid=USPAT4562374&id=v2QyAAAAEBAJ&oi=fnd&dq=Motor+device+utilizing+ultrasonic+oscillation&printsec=abstract#v=onepage&q=Motor%20device%20utilizing%20ultrasonic%20oscillation&f=false>.
- [2] SASHIDA T, KENJO T. *An introduction to ultrasonic motors*[M]. Oxford: Clarendon Press, 1993.
- [3] SHERRIT S. Smart material/actuator needs in extreme environments in space[C]//*Proceedings of the SPIE Smart Structure Conference*, San Diego, CA, May 20, 2005: 335-346.
- [4] UEHA S, TOMIKAWA Y. *Ultrasonic motors theory and applications*[M]. New York: Oxford Science Publications, 1993.
- [5] ZHAO C S. *Ultrasonic motors technologies and applications*[M]. Beijing: Science Press, 2010.
- [6] UCHINO K. *Piezoelectric actuator and ultrasonic motors*[M]. Boston, MA: Kluwer Academic Publishers, 1997.
- [7] HU J H, NAKAMURA K, UEHA S. An analysis of a noncontact ultrasonic motor with an ultrasonically levitated rotor[J]. *Ultrasonics*, 1997, 35(6): 459-467.
- [8] HU J H, NAKAMURA K, UEHA S. A noncontact ultrasonic motor with the rotor levitated by axial acoustic viscous force[J]. *Electronics and Communications in Japan (Part III)*, 1999, 82(4): 56-63.
- [9] IULA A, PAPPALARDO M. A high-power travelling wave ultrasonic motor[J]. *IEEE Transactions on Ultrasonics, Ferroelectrics, and Frequency Control*, 2006, 53(7): 1344-1351.
- [10] IULA A, CORBO A, PAPPALARDO M. FE analysis and experimental evaluation of the performance of a travelling wave rotary motor driven by high power ultrasonic transducers[J]. *Sensors and Actuators A: Physical*, 2010, 160(1-2): 94-100.

- [11] IULA A, BOLLINO G. A Travelling wave rotary motor driven by three pairs of Langevin transducers[J]. *IEEE Transactions on Ultrasonics, Ferroelectrics, and Frequency Control*, 2012, 59(1): 121–127.
- [12] SATONOBU J, FRIEND J R, NAKAMURA K, et al. Numerical analysis of the symmetric hybrid transducer ultrasonic motor[J]. *IEEE Transactions on Ultrasonics, Ferroelectrics and Frequency Control*, 2001, 48(6): 1 625–1 631.
- [13] JIN J M, ZHAO C S. A novel travelling wave ultrasonic motor using a bar shaped transducer[J]. *Journal of Wuhan University of Technology: Materials Science Edition*, 2008, 23(6): 961–963.
- [14] LIU Y X, CHEN W S, FENG P, et al. A square-type rotary ultrasonic motor with four driving feet[J]. *Sensors and Actuators A: Physical*, 2012, 180: 113–119.
- [15] LIU Y X, LIU J K, CHEN W S, et al. A cylindrical traveling wave ultrasonic motor using circumferential composite transducer[J]. *IEEE Transactions on Ultrasonics, Ferroelectrics, and Frequency Control*, 2011, 58(11): 2 397–2 404.
- [16] LIU Y X, CHEN W S, LIU J K, et al. Actuating mechanism and design of a cylindrical traveling wave ultrasonic motor using cantilever type composite transducer[J]. *PLoS ONE*, 2010, 5(4): e10020.
- [17] LIU Y X, CHEN W S, LIU J K, et al. A cylindrical traveling wave ultrasonic motor using longitudinal and bending composite transducer[J]. *Sensors and Actuators A: Physical*, 2010, 161(1–2): 158–163.
- [18] MORITA T, NIINO T, ASAMA H. Rotational feedthrough using ultrasonic motor for high vacuum condition[J]. *Vacuum*, 2002, 65 (1): 85–90.
- [19] PETIT L, GONNARD P. A multilayer TWILA ultrasonic motor[J]. *Sensors and Actuators A: Physical*, 2009, 149 (1): 113–119.
- [20] SHI Y L, LI Y B, ZHAO C S, et al. A new type butterfly-shaped transducer linear ultrasonic motor[J]. *Journal of Intelligent Material Systems and Structures*, 2011, 22(6): 567–575.
- [21] OR S W, CHAN H L W, LO V C, et al. Dynamics of an ultrasonic transducer used for wire bonding[J]. *IEEE Transactions on Ultrasonics, Ferroelectrics, and Frequency Control*, 1998, 45(6): 1453–1460.
- [22] XIAN X J, LIN S Y. Study on the compound multi-frequency ultrasonic transducer in flexural vibration[J]. *Ultrasonics*, 2008, 48(3): 202–208.

Biographical notes

LU Xiaolong, born in 1984, is currently a PhD candidate at *State Key Laboratory of Mechanics and Control of Mechanical Structures, Nanjing University of Aeronautics and Astronautics, China*. He received his ME degree from *Southeast University, China*, in 2009. His research interests include design and experiments of ultrasonic motors driven in extreme environments. Tel: +86-25-84893901; E-mail: long_8446110@nuaa.edu.cn

HU Junhui, born in 1965, is currently a professor at *Nanjing University of Aeronautics and Astronautics*. He received his PhD degree from *Tokyo Institute of Technology, Tokyo, Japan*, in 1997, and BE and ME degrees in electrical engineering from *Zhejiang University, Hangzhou, China*, in 1986 and 1989, respectively. He is a Chang-Jiang distinguished professor of *Ministry of Education of China*, director of *Precision Driving Lab at Nanjing University of Aeronautics and Astronautics (NUAA)*, and deputy director of *State Key Laboratory of Mechanics and Control of Mechanical Structures, China*. Tel: +86-25-84891681; E-mail: ejhhu@nuaa.edu.cn

YANG Lin, born in 1981, is currently a teacher at *State Key Laboratory of Mechanics and Control of Mechanical Structures, Nanjing University of Aeronautics and Astronautics, China*. He received his PhD degree from *Nanjing University of Aeronautics and Astronautics, China*, in 2010. His research interests include hybrid working mode ultrasonic motor design and fabrication. E-mail: yanglin@nuaa.edu.cn

ZHAO Chunsheng, born in 1938, is currently a professor at *State Key Laboratory of Mechanics and Control of Mechanical Structures, Nanjing University of Aeronautics and Astronautics (NUAA), Nanjing, China*. He is the founder of *Precision Driving Laboratory at NUAA*, and an academician of *Chinese Academy of Sciences*. He holds 54 patents in China and has published more than 400 papers in the field of ultrasonic motors. Tel: +86-25-84896661; E-mail: cszhao@nuaa.edu.cn